Heliyon 9 (2023) e13121

Contents lists available at ScienceDirect

Heliyon

journal homepage: www.cell.com/heliyon

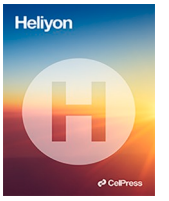

Research article

Spatiotemporal characteristics of dynamic speckle from a 3D target in atmospheric turbulence

Wang Liguo *, Gong Lei, Li Yaqing, Yang Zhiqiang, Yang Lihong, Li Yao

School of Photoelectrical Engineering, Xi'an Technological University, Xi'an, 710021, China

ARTICLE INFO

Keywords:
Atmospheric turbulence
Dynamic speckle
3D target
Spatiotemporal correlation function

ABSTRACT

Spatiotemporal correlation function is the basic characteristic of dynamic laser speckle and the basis of various applications. The correlation function of the speckle intensity from a 3D target in turbulent atmosphere is derived based on the model of random phase screen and Fresnel Kirchhoff Diffraction Formula, and a fast algorithm based on FFT is developed. The particularity of dynamic speckle in turbulence is numerically analyzed and discussed. The results show that the speckle intensity fluctuates at two independent scales both in space and time domain, which are affected by target size and atmospheric turbulence respectively. In particular, the time scale caused by turbulence is also affected by the target translating velocity and the wind direction. The theory and algorithm developed in this paper can play important roles in applications of laser speckle such as remote detection in atmospheric environment.

1. Introduction

Various technologies based on laser speckle have been developed to detect the shape [1], velocity [2], deformation [3] or other physical properties of a remote object. Due to the randomness of the speckle field, most of these technologies are based on the statistics characteristics of the speckle field, such as the spatial and temporal correlation functions, which have been researched for various types of targets since the 1970s by scholars all over the world [4–6].

In the recent decades, spatiotemporal correlation function of speckle field in the cases of different types of targets had been a hot point. In 2008, American scholar Yura researched the spatiotemporal intensity covariance function of scattering field from a plane target illuminated by multiple laser beams [7]. In 2013, Zhang Geng researched the same function in the case of a 3D cyclotron target based on Kirchhoff approximation [8]. In 2017, Sun Tianjing studied the spatio-temporal cross-correlation function of dynamic speckle from a rough plane illuminated by an ultrafast laser beam theoretically and experimentally [9].

These researches are mainly based on the translation of the fourth-order statistical moment of the speckle field into the sum of second-order moments, while assuming that the field is complex Gaussian random. However, the translation would be invalid in some cases, such as when the laser light propagates through the turbulent atmosphere. The departure from the Gaussian distribution of the speckle field demands direct research on the fourth moment. Scholars from the former Soviet Union and the United States had studied this problem in an earlier time, and had established the models of speckle field from various types of targets, such as point scatterers, rough plate disks, mirrors, retroreflectors, in a turbulent environment [10–14]. Since the beginning of the new century, researches on the speckle field in atmospheric turbulence have been gradually expanding to more complex situations. In 2008, Wei Hongyan studied

* Corresponding author.
E-mail address: kinglywang3773@163.com (W. Liguo).

https://doi.org/10.1016/j.heliyon.2023.e13121
Received 21 September 2022; Received in revised form 12 January 2023; Accepted 17 January 2023
Available online 21 January 2023

the double-pass propagation of laser beams along slant paths in atmosphere, and deduced the covariance function of speckle intensity [15]. In 2018, Jia Li experimentally measured the average intensity and correlation function affected by the backward enhancement effect during the double-passage of the laser beam in non-classical turbulence [16]. Olga korotkova conducted theoretical and Numerical researches on the backward enhancement effect of laser light scattered by a retroreflector in the marine turbulence [17]. The authors of this paper have been committed to the research on speckle field in turbulent atmosphere, and have studied the four-order moments of the speckle field from targets such as set of point scatterer [18], hard-edge aperture plane targets [19] and particle cluster [20] in turbulent atmosphere in recent years. However, the characteristics of spatiotemporal correlation of the speckle from a 3D target with arbitrary shape have not been perfectly solved.

In this paper, the expression of correlation function of the speckle intensity from a 3D rough target in atmospheric turbulence is derived, and a fast algorithm of the expression is proposed. Taking a Lambertian cylinder as an example, the influence of turbulence on the normalized covariance function of the speckle intensity from a 3D target is numerically analyzed, and the temporal and spatial distribution of the normalized variance of the speckle intensity is discussed.

2. Theoretical model of the spatiotemporal correlation function of speckle intensity

2.1. Correlation function of speckle intensity from a rough plane target

Fig. 1 describes an optical system that generates speckle field without considering turbulence, where the target is a quadrilateral rough plane moving in an arbitrary way and is illuminated by a laser beam. A coordinate system is established with its origin point at the center of the emitting aperture of the laser beam and z axis along the beam axis. The target is located above the emitter and not far from z axis, and the position on the target is represented by a 3D coordinate $\boldsymbol{\rho} = (\rho_x, \rho_y, \rho_z)$. The receiving point is located around the origin, being represented by a 3D coordinate $\mathbf{p} = (p_x, p_y, p_z)$. The normal direction of the target surface is $\hat{\mathbf{n}}$, pointing to the side irradiated by the laser. The speed of the target point $\boldsymbol{\rho}$ is $\mathbf{V}$.

If the target is remote, the wavefront of the transmitted wave can be approximated as a spherical wave, the curvature center of the wavefront can be approximated seen at transmitting point, and the field reaching the target surface can be expressed as Equation 1

$$U_i(\boldsymbol{\rho}) = U_0 \exp(ik|\boldsymbol{\rho}|) \tag{1}$$

The model of random phase screen can be adopted to simulate the rough plane surface, which means that the main influence of the target on the incident field is adding a random phase associating with the random fluctuation of the surface height. Based on the Fresnel-Kirchhoff diffraction formula [21], the scattered field of the target at the time t can be expressed as Equation 2

$$U_{sp}(\mathbf{p}, t) = C \int_S d\boldsymbol{\rho} U_i(\boldsymbol{\rho}) \cos\theta_i \exp[ik(\cos\theta_i + \cos\theta_s)\zeta(\boldsymbol{\rho} - \mathbf{V}t)] \frac{\exp(ik|\mathbf{p} - \boldsymbol{\rho}|)}{|\mathbf{p} - \boldsymbol{\rho}|} \tag{2}$$

where C is a constant, $\zeta(\boldsymbol{\rho})$ is the height fluctuation of the target surface, θ_i and θ_s are the incidence and the scattering angles which can be expressed as Equation 3

$$\begin{aligned} \cos(\theta_i) &= -\boldsymbol{\rho} \cdot \hat{\mathbf{n}}/\rho \\ \cos(\theta_s) &= (\mathbf{p} - \boldsymbol{\rho}) \cdot \hat{\mathbf{n}}/|\mathbf{p} - \boldsymbol{\rho}| \end{aligned} \tag{3}$$

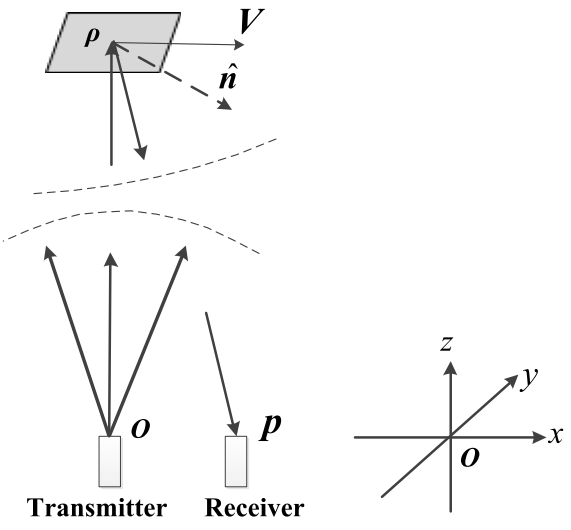

Fig. 1. Geometric diagram of the optical system generating speckle field by a plane target in the absence of turbulence.

Because the target size and the distance between the receiving point and the transmitting point are both much smaller than the distance from the target to the transmitting point, the incident angle and scattering angle are approximately equal and unchanged with the incidence position on the target, the value of the angles can be written as Equation 4

$$\theta_s \approx \theta_i \approx \arccos(-\boldsymbol{\rho}_0 \cdot \hat{\mathbf{n}} / \rho_0) \tag{4}$$

where $\boldsymbol{\rho}_0$ is the center of the target.

Making the transformation $\boldsymbol{\rho}' = \boldsymbol{\rho} - \mathbf{V}t$, the speckle field becomes

$$U_{sp}(\mathbf{p},t) = C\int_{S'} d\boldsymbol{\rho}' U_0 \exp\left(ik\left|\boldsymbol{\rho}'_n + \mathbf{V}t\right|\right)\cos\theta_i \exp[i2k\cos\theta_i\zeta(\boldsymbol{\rho}')]\frac{\exp\left(ik\left|\mathbf{p}-\boldsymbol{\rho}'_n-\mathbf{V}t\right|\right)}{\left|\mathbf{p}-\boldsymbol{\rho}'_n-\mathbf{V}t\right|} \tag{5}$$

To simplify the calculation of Equation (5), it is necessary to further approximate the above formula. Due to the large propagating distance, the attenuation factors of the waves scattered by different points on the target are approximately the same when they reach the receiving point. Furthermore, only a very short period of time needs to be considered when the time correlation of the speckle is studied, because the time correlation of the speckle declines rapidly for a moving target. The gesture and position of the target can also be approximately seen as unchanged in the period. The amplitude attenuation factor can be written as Equation 6

$$\frac{1}{\left|\mathbf{p}-\boldsymbol{\rho}'_n-\mathbf{V}t\right|} \simeq \frac{1}{z'_0} \tag{6}$$

where z'_0 is the z coordinate of the target center.

Using first order approximation, the phase terms in Equation (5) can be written as Equations (7) and (8)

$$\exp(ik|\boldsymbol{\rho}' + \mathbf{V}t|) = \exp(ikz' + ikV_z t)\exp\left(ik\frac{\left|\boldsymbol{\rho}'_{xy}\right|^2 + 2\boldsymbol{\rho}'_{xy}\cdot\mathbf{V}_{xy}t + \left|\mathbf{V}_{xy}t\right|^2}{2z'_0}\right) \tag{7}$$

$$\exp(ik|\mathbf{p}-\boldsymbol{\rho}' - \mathbf{V}t|) = \exp(ikz' + ikV_z t)\exp\left[ik\frac{\left|\mathbf{p}_{xy}-\boldsymbol{\rho}'_{xy}\right|^2 - 2\left(\mathbf{p}_{xy}-\boldsymbol{\rho}'_{xy}\right)\cdot\mathbf{V}_{xy}t + \left|\mathbf{V}_{xy}t\right|^2}{2z'_0}\right] \tag{8}$$

where z' is the z coordinate of the target point $\boldsymbol{\rho}'$, $\boldsymbol{\rho}'_{xy}$ is the component of vector $\boldsymbol{\rho}'$ on the x-y plane. V_z and $\mathbf{V}_{xy}$ are speed components of the $\boldsymbol{\rho}'$ point respectively along the z axes and on x-y plane, which are approximately unchanged in the short period.

Using Equations (6)–(6)–(8) in Equation (5), the speckle field can be expressed as Equation 9

$$\begin{aligned} U_{sp}(\mathbf{p},t) &= \frac{C}{z'_0}\int_{S'} d\boldsymbol{\rho}' U_0 \cos\theta_i \exp[i2k\cos\theta_i\zeta(\boldsymbol{\rho}')]\exp(i2kz' + ikV_z t) \\ &\times\exp\left(ik\frac{\left|\mathbf{p}_{xy}-\boldsymbol{\rho}'_{xy}\right|^2 + \left|\boldsymbol{\rho}'_{xy}\right|^2}{2z'_0} + ik\frac{\left(2\boldsymbol{\rho}'_{xy}-\mathbf{p}_{xy}\right)\cdot\mathbf{V}_{xy}t}{z'_0} + ik\frac{\left|\mathbf{V}_{xy}t\right|^2}{z'_0}\right) \end{aligned} \tag{9}$$

Then we can get the spatiotemporal correlation function of the plane target

$$\begin{aligned} \Gamma(\mathbf{p}_1,\mathbf{p}_2,\tau) &= \langle U'_{sp}\left(\mathbf{p}_1, -\frac{\tau}{2}\right)U'^{*}_{sp}\left(\mathbf{p}_2,\frac{\tau}{2}\right)\rangle \\ &= \frac{C^2U_0^2}{z'^2_0}\int_{S'}\int_{S'}(\cos\theta_i)^2\langle\exp\left\{i2k\cos\theta_i\left[\zeta\left(\boldsymbol{\rho}'_1\right)-\zeta\left(\boldsymbol{\rho}'_2\right)\right]\right\}\rangle \\ \times\exp\left[i2k\left(z'_1-z'_2\right)-ik\tau\left(V_{z1}+V_{z2}\right)\right]&\exp\left(ik\frac{\left|\mathbf{p}_{xy1}-\boldsymbol{\rho}'_{xy1}\right|^2+\left|\boldsymbol{\rho}'_{xy1}\right|^2}{2z'_0}-ik\frac{\left|\mathbf{p}_{xy2}-\boldsymbol{\rho}'_{xy2}\right|^2+\left|\boldsymbol{\rho}'_{xy2}\right|^2}{2z'_0}\right) \\ \times\exp\left[-ik\frac{\tau}{2}\frac{\left(2\boldsymbol{\rho}'_{xy1}-\mathbf{p}_{xy1}\right)\cdot\mathbf{V}_{xy1}+\left(2\boldsymbol{\rho}'_{xy2}-\mathbf{p}_{xy2}\right)\cdot\mathbf{V}_{xy2}}{z'_0}\right]&\exp\left(ik\frac{\left|\mathbf{V}_{xy1}\frac{\tau}{2}\right|^2-\left|\mathbf{V}_{xy2}\frac{\tau}{2}\right|^2}{z'_0}\right)d\boldsymbol{\rho}'_1 d\boldsymbol{\rho}'_2 \end{aligned} \tag{10}$$

The height fluctuations on a rough surface meet Equation 11

$$\langle\exp\left\{i2k\cos\theta_i\left[\zeta\left(\boldsymbol{\rho}'_1\right)-\zeta\left(\boldsymbol{\rho}'_2\right)\right]\right\}\rangle = \exp\left\{-2k(\cos\theta_i)^2\sigma^2\left[1-\mathrm{c}\left(\boldsymbol{\rho}'_1-\boldsymbol{\rho}'_2\right)\right]\right\} \tag{11}$$

where σ and $\mathrm{c}(\boldsymbol{\rho}'_1-\boldsymbol{\rho}'_2)$ are the RMS and normalized correlation function of the height fluctuation, respectively [21].

By making the variables substitution defined by Equation 12

$$\boldsymbol{\rho}'_- = \boldsymbol{\rho}'_1 - \boldsymbol{\rho}'_2, \boldsymbol{\rho}'_+ = \left(\boldsymbol{\rho}'_1 + \boldsymbol{\rho}'_2\right)/2 \tag{12}$$

Equation (10) can be translated into Equation 13

$$\Gamma(\mathbf{p}_1,\mathbf{p}_2,\tau)=\frac{C^2U_0^2}{z_0'^2}\int_{S_-'}\int_{S_+'}(\cos\theta_i)^2\exp\{-2k(\cos\theta_i)^2\sigma^2[1-\mathrm{c}(\boldsymbol{\rho}_1'-\boldsymbol{\rho}_2')]\}\exp[i2kz_-']$$
$$\times\exp\left(ik\frac{|\mathbf{p}_{xy1}|^2-|\mathbf{p}_{xy2}|^2-2(\mathbf{p}_{xy1}-\mathbf{p}_{xy2})\cdot\boldsymbol{\rho}_{+xy}'-(\mathbf{p}_{xy1}+\mathbf{p}_{xy2})\cdot\boldsymbol{\rho}_{-xy}'+4\boldsymbol{\rho}_{-xy}'\cdot\boldsymbol{\rho}_{+xy}'}{2z_0'}\right)$$
$$\times\exp\left[-ik\tau 2V_z-ik\tau\frac{4(\boldsymbol{\rho}_{+xy}')\cdot\mathbf{V}_{xy}-(\mathbf{p}_{xy1}+\mathbf{p}_{xy2})\cdot\mathbf{V}_{xy}}{2z_0'}\right]d\boldsymbol{\rho}_-'d\boldsymbol{\rho}_+' \tag{13}$$

where S_+' is the integral region of the variable $\boldsymbol{\rho}_+'$, which is equal to the illuminated region on the target. As the integral about $\boldsymbol{\rho}_+'$ is a function of $\boldsymbol{\rho}_{+xy}'$, the component on x-y plane, the variable substitution $d\boldsymbol{\rho}_{+xy}'/\cos\theta_i=d\boldsymbol{\rho}_+'$ can be introduced with the new integral region S_{+xy}' being the projection of S_+' on x-y plane. S_-' is the integral region of the variable $\boldsymbol{\rho}_-'$. For most rough surface, σ is larger than the wavelength and $\mathrm{c}(\boldsymbol{\rho}_-')$ falls rapidly to zero when $|\boldsymbol{\rho}_-'|$ exceeds the correlation length which is usually much smaller than the size of the target, so S_-' can be extended to infinite without any influence on the result of the integral. It is also because that the correlation region is small enough that the effect of transverse component of $\boldsymbol{\rho}_-'$ on the phase terms can be neglected. Then the correlation function becomes Equation 14

$$\begin{aligned}\Gamma(\mathbf{p}_1,\mathbf{p}_2,\tau)=&\frac{C^2U_0^2}{z_0'^2}\cos\theta_i\exp\left[-ik\tau 2V_z+ik\frac{(\mathbf{p}_{xy1}+\mathbf{p}_{xy2})\cdot\mathbf{V}_{xy}\tau+|\mathbf{p}_{xy1}|^2-|\mathbf{p}_{xy2}|^2}{2z_0'}\right]\\&\times\int_\infty\exp\{-2k(\cos\theta_i)^2\sigma^2\mathrm{c}(\boldsymbol{\rho}_-')\}\exp[i2kz_-']d\boldsymbol{\rho}_-'\\&\times\int_{S_{+xy}'}\exp\left(-ik\frac{(\mathbf{p}_{xy1}-\mathbf{p}_{xy2})\boldsymbol{\rho}_{+xy}'+2\boldsymbol{\rho}_{+xy}'\cdot\mathbf{V}_{xy}\tau}{z_0'}\right)d\boldsymbol{\rho}_{+xy}'\end{aligned} \tag{14}$$

It can be seen that Equation (14) contains three parts. The first part contains the terms that independent with variables $\boldsymbol{\rho}_+'$ and $\boldsymbol{\rho}_-'$. The second part is the integral about $\boldsymbol{\rho}_-'$ which is related to the mean intensity of the field. In fact, the mean intensity can be written as Equation 15

$$\langle I_s\rangle=\Gamma(\mathbf{p},\mathbf{p},0)=\frac{C^2U_0^2S}{z_0'^2}(\cos\theta_i)^2\int_\infty\exp\{-2k(\cos\theta_i)^2\sigma^2\mathrm{c}(\boldsymbol{\rho}_-')\}\exp[i2kz_-']d\boldsymbol{\rho}_- \tag{15}$$

In another way, the mean intensity can be expressed by Bidirectional Reflectance Distribution Function (BRDF)

$$\langle I_s\rangle=\Gamma(\mathbf{p},\mathbf{p},0)=\frac{U_0^2S}{z_0'^2}(\cos\theta_i)^2\mathrm{brdf}(\theta_i,0;\theta_i\ ,\ \ \pi) \tag{16}$$

Comparing Equations (15) and (16), we can get the relationship in Equation 17

$$\int_\infty\exp\{-2k(\cos\theta_i)^2\sigma^2\mathrm{c}(\boldsymbol{\rho}_-')\}\exp[i2kz_-']d\boldsymbol{\rho}_-'=\frac{1}{C^2}\mathrm{brdf}(\theta_i,0;\theta_i\ ,\ \ \pi) \tag{17}$$

The brdf is usually more accessible than the height fluctuation of a surface, so we choose using brdf to describe the scattering characteristic of the target surface in the following passage

$$\begin{aligned}\Gamma(\mathbf{p}_1,\mathbf{p}_2,\tau)=&\frac{U_0^2}{z_0'^2}\cos\theta_i\exp\left[-ik\tau 2V_z+ik\frac{(\mathbf{p}_{xy1}+\mathbf{p}_{xy2})\cdot\mathbf{V}_{xy}\tau+|\mathbf{p}_{xy1}|^2-|\mathbf{p}_{xy2}|^2}{2z_0'}\right]\\&\times\mathrm{brdf}(\theta_i,0;\theta_i\ ,\ \ \pi)\int_{S_{+xy}'}\exp\left(-ik\frac{(\mathbf{p}_{xy1}-\mathbf{p}_{xy2})\boldsymbol{\rho}_{+xy}'+2\boldsymbol{\rho}_{+xy}'\cdot\mathbf{V}_{xy}\tau}{z_0'}\right)d\boldsymbol{\rho}_{+xy}'\end{aligned} \tag{18}$$

Assuming that the projection of the target on the x-y plane is a rectangle with length of Δx and width of Δy respectively and with the center at $\boldsymbol{\rho}_{xy0}'$, the analytical form of spatiotemporal correlation function in Equation (19) can be obtained by completing the integration in Equation 18

$$\begin{aligned}&\Gamma(\mathbf{p}_1,\mathbf{p}_2,\tau)\\=&\frac{U_0^2S_{xy}}{z_0'^2}\cos\theta_i\mathrm{brdf}(\theta_i,0;\theta_i\ ,\ \ \pi)\exp\left(ik\frac{|\mathbf{p}_{xy1}|^2-|\mathbf{p}_{xy2}|^2}{2z_0'}+ik\mathbf{V}_{xy}\cdot(\mathbf{p}_{xy1}+\mathbf{p}_{xy2})\frac{\tau}{2z_0'}-i2kV_z\tau\right)\\&\times\exp\left[-ik\frac{(\mathbf{p}_{xy1}-\mathbf{p}_{xy2}+2\mathbf{V}_{xy}\tau)\cdot\boldsymbol{\rho}_{xy0}'}{z_0'}\right]\mathrm{sinc}2\left[\frac{S_{xy}}{\lambda z_0'}(\mathbf{p}_{xy1}-\mathbf{p}_{xy2}+2\mathbf{V}_{xy}\tau)\right]\end{aligned} \tag{19}$$

where $S_{xy}=\Delta x\Delta y=S\cos\theta_i$, sinc2 is the two dimension sinc function

2.2. Correlation function of speckle intensity from a 3D target in atmospheric turbulence

In this section, we build the model of speckle field from a 3D target with all or part of the light propagation being in atmospheric turbulence as shown in Fig. 2. The coordinate system is similar to the one in Fig. 1. The laser propagates through the atmosphere, irradiates the 3D target with rough surface. The scattered light returns to the receiver near the transmitter to form the speckle field.

The smallest rectangular region which can cover the projection of the target on the x-y plane is divided into rectangular meshes. Then the irradiated region of the target can be divided into quadrilateral facets corresponding to the meshes. The scattered field from the target can be expressed by the superposition of the field from all facets as Equation 20

$$U_s(\mathbf{p},t)=\sum_{n=1}^{N}U_{sn}(\mathbf{p},t) \tag{20}$$

where U_{sn} is the field from the nth facet,

$$\begin{aligned}U_{sn}(\mathbf{p},t)=C\int_{Sn}U_0\exp(ik|\boldsymbol{\rho}|)\exp[\psi_i(\boldsymbol{\rho})]\cos\theta_i\exp[ik(\cos\theta_i+\cos\theta_s)\zeta(\boldsymbol{\rho}-\mathbf{V}t)]\\ \times\frac{\exp(ik|\mathbf{p}-\boldsymbol{\rho}|)}{|\mathbf{p}-\boldsymbol{\rho}|}\exp[\psi_R(\boldsymbol{\rho},\mathbf{p})]d\boldsymbol{\rho}\end{aligned} \tag{21}$$

where $\psi_i(\boldsymbol{\rho})$ and $\psi_R(\boldsymbol{\rho},\mathbf{p})$ are the complex perturbations of turbulence on light propagating along the forward and backward paths, respectively.

Making sure that sizes of the facets are small enough so that the influence of turbulence on the incident and scattered light from all points on a facet is basically consistent, and using variable substitution $\boldsymbol{\rho}'=\boldsymbol{\rho}-Vt$, Equation (21) can be transformed into Equation 22

$$\begin{aligned}U_{sn}(\mathbf{p},t)&=\exp\left[\psi_i\left(\boldsymbol{\rho}'_{n0}+\mathbf{V}_{n0}t\right)+\psi_R\left(\boldsymbol{\rho}'_{n0}+\mathbf{V}_{n0}t,\mathbf{p}\right)\right]\\ \times C\int_{S'n}U_0\exp(ik|\boldsymbol{\rho}'+\mathbf{V}t|)\cos\theta_i\exp[ik(\cos\theta_i+\cos\theta_s)\zeta(\boldsymbol{\rho}')]\frac{\exp(ik|\mathbf{p}-\boldsymbol{\rho}'-\mathbf{V}t|)}{|\mathbf{p}-\boldsymbol{\rho}'-\mathbf{V}t|}d\boldsymbol{\rho}'\\ &=T_n(\mathbf{p},t)U'_{sn}(\mathbf{p},t)\end{aligned} \tag{22}$$

where $T_n(\mathbf{p},t)$ is the turbulence effect on the scattered wave from the central point $\boldsymbol{\rho}_{n0}$ of the nth facet, $U'_{sn}(\mathbf{p},t)$ is the field from the nth facet in the absence of turbulence.

The spatio-temporal correlation function of the scattered intensity from the target is defined by Equation 23

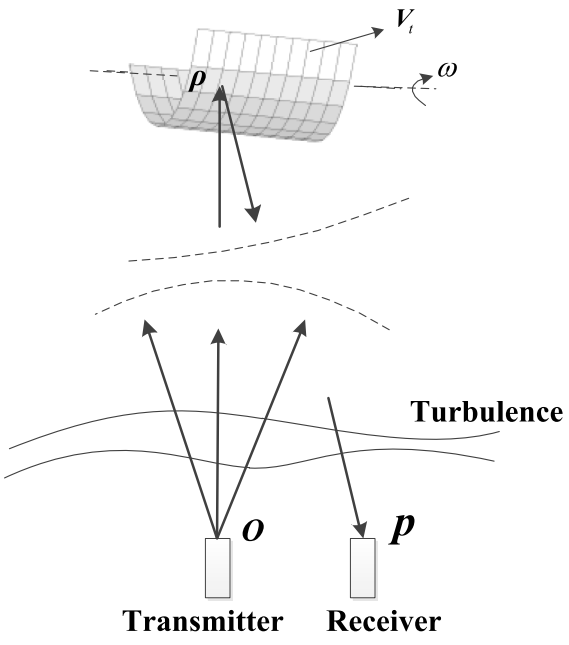

Fig. 2. Geometric diagram of the system generating speckle field by a 3D target in the presence of turbulence.

$$
\begin{aligned}
B_I(\mathbf{p}_1,\mathbf{p}_2,\tau) &= \langle I\left(\mathbf{p}_1,-\frac{\tau}{2}\right)I\left(\mathbf{p}_2,\frac{\tau}{2}\right)\rangle = \langle U_s\left(\mathbf{p}_1,-\frac{\tau}{2}\right)U_s^*\left(\mathbf{p}_1,-\frac{\tau}{2}\right)U_s\left(\mathbf{p}_2,\frac{\tau}{2}\right)U_s^*\left(\mathbf{p}_2,\frac{\tau}{2}\right)\rangle \\
&= \langle \sum_{n=1}^{N}\sum_{n'=1}^{N}\sum_{m=1}^{N}\sum_{m'=1}^{N} T_n\left(\mathbf{p}_1,-\frac{\tau}{2}\right)U'_{sn}\left(\mathbf{p}_1,-\frac{\tau}{2}\right)T^*_{n'}\left(\mathbf{p}_1,-\frac{\tau}{2}\right)U'^*_{sn'}\left(\mathbf{p}_1,-\frac{\tau}{2}\right)T_m\left(\mathbf{p}_2,\frac{\tau}{2}\right)U'_{sm}\left(\mathbf{p}_2,\frac{\tau}{2}\right)T^*_{m'}\left(\mathbf{p}_2,\frac{\tau}{2}\right)U'^*_{sm'}\left(\mathbf{p}_2,\frac{\tau}{2}\right)\rangle \\
&= \sum_{n=1}^{N}\sum_{n'=1}^{N}\sum_{m=1}^{N}\sum_{m'=1}^{N}\langle T_n\left(\mathbf{p}_1,-\frac{\tau}{2}\right)T^*_{n'}\left(\mathbf{p}_1,-\frac{\tau}{2}\right)T_m\left(\mathbf{p}_2,\frac{\tau}{2}\right)T^*_{m'}\left(\mathbf{p}_2,\frac{\tau}{2}\right)\rangle\langle U'_{sn}\left(\mathbf{p}_1,-\frac{\tau}{2}\right)U'^*_{sn'}\left(\mathbf{p}_1,-\frac{\tau}{2}\right)U'_{sm}\left(\mathbf{p}_2,\frac{\tau}{2}\right)U'^*_{sm'}\left(\mathbf{p}_2,\frac{\tau}{2}\right)\rangle
\end{aligned}
\tag{23}
$$

Each facet contains a large number of scattering centers, and its speckle field in the absence of turbulence is complex Gaussian random, thus the fourth-order moment of the speckle field from the panels can be expressed as Equation 24

$$
\begin{aligned}
&\langle U'_{sn}\left(\mathbf{p}_1,-\frac{\tau}{2}\right)U'^*_{sn'}\left(\mathbf{p}_1,-\frac{\tau}{2}\right)U'_{sm}\left(\mathbf{p}_2,\frac{\tau}{2}\right)U'^*_{sm'}\left(\mathbf{p}_2,\frac{\tau}{2}\right)\rangle \\
&= \langle U'_{sn}\left(\mathbf{p}_1,-\frac{\tau}{2}\right)U'^*_{sn'}\left(\mathbf{p}_1,-\frac{\tau}{2}\right)\rangle\langle U'_{sm}\left(\mathbf{p}_2,\frac{\tau}{2}\right)U'^*_{sm'}\left(\mathbf{p}_2,\frac{\tau}{2}\right)\rangle \\
&+\langle U'_{sn}\left(\mathbf{p}_1,-\frac{\tau}{2}\right)U'^*_{sm'}\left(\mathbf{p}_2,\frac{\tau}{2}\right)\rangle\langle U'_{sm}\left(\mathbf{p}_2,\frac{\tau}{2}\right)U'^*_{sn'}\left(\mathbf{p}_1,-\frac{\tau}{2}\right)\rangle
\end{aligned}
\tag{24}
$$

The speckle field from different facets is unrelated, which means

$$
\langle U'_{sn}(\mathbf{p}_1,t_1)U'^*_{sm}(\mathbf{p}_2,t_2)\rangle = \delta(n-m)\Gamma_{nn}(\mathbf{p}_1,\mathbf{p}_2,t_2-t_1) \tag{25}
$$

where $\Gamma_{nn}(\mathbf{p}_1,\mathbf{p}_2,t_2-t_1)$ is the correlation function of the speckle field from a plane target described in Equation (19).

Substituting Equations (24) and (25) in Equation (23), the correlation function of the received intensity can be transformed into Equation 26

$$
\begin{aligned}
B_I(\mathbf{p}_1,\mathbf{p}_2,\tau) &= \sum_{n=1}^{N}\sum_{m=1}^{N} I_nI_m\langle T_n\left(\mathbf{p}_1,-\frac{\tau}{2}\right)T^*_n\left(\mathbf{p}_1,-\frac{\tau}{2}\right)T_m\left(\mathbf{p}_2,\frac{\tau}{2}\right)T^*_m\left(\mathbf{p}_2,\frac{\tau}{2}\right)\rangle \\
&+\sum_{n=1}^{N}\sum_{m\neq n}^{N}\Gamma^4(\mathbf{p}_1,\mathbf{p}_2,\tau)\langle T_n\left(\mathbf{p}_1,-\frac{\tau}{2}\right)T^*_n\left(\mathbf{p}_2,\frac{\tau}{2}\right)T_m\left(\mathbf{p}_2,\frac{\tau}{2}\right)T^*_m\left(\mathbf{p}_1,-\frac{\tau}{2}\right)\rangle
\end{aligned}
\tag{26}
$$

where $I_n = \Gamma_{nn}(\mathbf{p}_1,\mathbf{p}_1,0)$ is the mean intensity from the nth facet, $\Gamma^4(\mathbf{p}_1,\mathbf{p}_2,\tau) = \Gamma_{nn}(\mathbf{p}_1,\mathbf{p}_2,\tau)\Gamma^*_{mm}(\mathbf{p}_1,\mathbf{p}_2,\tau)$ is the fourth order moment of the speckle field of the nth facet in the absence of turbulence.

Since the propagating distance is much larger than the target size, the z coordinates of the centers of all the facets are approximately the same, which means $z'_{n0} \simeq z'_{m0} \simeq L$, where L is the mean distance from the emitting center to the illuminated region. Then the fourth order moment can be simplified as Equation 27

$$
\begin{aligned}
&\Gamma^4(\mathbf{p}_1,\mathbf{p}_2,\tau) = \\
&= I_nI_m\exp\left[-ik\frac{(\mathbf{p}_{xy1}-\mathbf{p}_{xy2})\cdot\left(\boldsymbol{\rho}'_{xyn}-\boldsymbol{\rho}'_{xym}\right)}{L}+ik\frac{(\mathbf{p}_{xy1}+\mathbf{p}_{xy2})\cdot(\mathbf{V}_{xyn}-\mathbf{V}_{xym})\tau}{2L}\right] \\
&\times\exp\left[-ik\frac{2\left(\boldsymbol{\rho}'_{xyn}\cdot\mathbf{V}_{xyn}-\boldsymbol{\rho}'_{xym}\cdot\mathbf{V}_{xym}\right)\tau}{L}-i2k(V_{zn}-V_{zm})\tau\right] \\
&\times\mathrm{sinc2}\left[\frac{S_{xy}}{\lambda L}(\mathbf{p}_{xy1}-\mathbf{p}_{xy2}+2\mathbf{V}_{xyn}\tau)\right]\mathrm{sinc2}\left[\frac{S_{xy}}{\lambda L}(\mathbf{p}_{xy1}-\mathbf{p}_{xy2}+2\mathbf{V}_{xym}\tau)\right]
\end{aligned}
\tag{27}
$$

As S_{xy} is small, the two sinc2 functions vary slowly relative to the phase terms in Equation (27), which means that the phase terms play a leading role in the variation of the correlation function of the scattered intensity from the whole target. Therefore, the sinc2 functions can be neglected while calculating $B_I(\mathbf{p}_1,\mathbf{p}_2,\tau)$, and Equation (27) is simplified as Equation 28

$$
\begin{aligned}
&\Gamma^4(\mathbf{p}_1,\mathbf{p}_2,\tau) \\
&= I_nI_m\exp\left[-ik\frac{(\mathbf{p}_{xy1}-\mathbf{p}_{xy2})\cdot\left(\boldsymbol{\rho}'_{xyn}-\boldsymbol{\rho}'_{xym}\right)}{L}+ik\frac{(\mathbf{p}_{xy1}+\mathbf{p}_{xy2})\cdot(\mathbf{V}_{xyn}-\mathbf{V}_{xym})\tau}{2L}\right] \\
&\times\exp\left[-ik\frac{2\left(\boldsymbol{\rho}'_{xyn}\cdot\mathbf{V}_{xyn}-\boldsymbol{\rho}'_{xym}\cdot\mathbf{V}_{xym}\right)\tau}{L}-i2k(V_{zn}-V_{zm})\tau\right]
\end{aligned}
\tag{28}
$$

In a short period, any motion of the rigid target can be decomposed into a translational motion and a rotational motion around an axis. Assuming that the translational velocity is $\mathbf{V}_t$ and the angular velocity is ω with the rotation axis passing through the point $\boldsymbol{\rho}_e = (\rho_{ex},\rho_{ey},\rho_{ez})$ and pointing along the direction $\hat{\mathbf{r}} = (r_x,r_y,r_z)$, the instantaneous velocity of a target point $\boldsymbol{\rho}' = (\rho'_x,\rho'_y,\rho'_z)$ is expressed as Equation 29

$$\begin{aligned}\mathbf{V} &= \mathbf{V}_t + \mathbf{V}_r = \mathbf{V}_t + \widehat{\mathbf{r}} \times (\boldsymbol{\rho}' - \boldsymbol{\rho}_e) \\ &= \left[V_{tx} + r_y(\rho_z' - \rho_{ez}) - r_z\left(\rho_y' - \rho_{ey}\right)\right]\widehat{\mathbf{x}} - \left[V_{ty} + r_x(\rho_z' - \rho_{ez}) - r_z(\rho_x' - \rho_{ex})\right]\widehat{\mathbf{y}} \\ &\quad + \left[V_{tz} + r_x\left(\rho_y' - \rho_{ey}\right) - r_y(\rho_x' - \rho_{ex})\right]\widehat{\mathbf{z}}\end{aligned} \tag{29}$$

Substituting Equation (29) into Equation (28), the fourth order moment of the speckle field in the absence of turbulence becomes Equation 30

$$\begin{aligned}&\Gamma^4(\mathbf{p}_1, \mathbf{p}_2, \tau) \\ &= I_n I_m \exp\left[- ik\frac{(\mathbf{p}_{xy1} - \mathbf{p}_{xy2}) \cdot \left(\boldsymbol{\rho}_{xyn}' - \boldsymbol{\rho}_{xym}'\right)}{L} - ik\frac{2\left(\boldsymbol{\rho}_{xyn}' \cdot \mathbf{V}_{txy} - \boldsymbol{\rho}_{xym}' \cdot \mathbf{V}_{txy}\right)\tau}{L}\right] \\ &\times \exp\left[ik\frac{(\mathbf{p}_{xy1} + \mathbf{p}_{xy2}) \cdot (\mathbf{V}_{rxyn} - \mathbf{V}_{rxym})\tau}{2L} - ik\frac{2\left(\boldsymbol{\rho}_{xyn}' \cdot \mathbf{V}_{rxyn} - \boldsymbol{\rho}_{xym}' \cdot \mathbf{V}_{rxym}\right)\tau}{L} - i2k(V_{rzn} - V_{rzm})\tau\right]\end{aligned} \tag{30}$$

Except the case that the rotation axis of the target points around the receiving region or the *n*th and *m*th facet are both across the plane defined by the rotation axis and the scattering direction, the velocity components along each direction are on the same order in most situations. As the first two phase terms caused by the rotational motion contains L as denominators, they usually are much smaller than the last phase term, which means that the influence of the velocity components parallel to the x-y plane can be neglected. Thus, Equation (30) can be simplified into Equation 31

$$\Gamma^4(\mathbf{p}_1, \mathbf{p}_2, \tau) = I_n I_m \exp\left[- \frac{ik}{L}\left(\mathbf{p}_{xy1} - \mathbf{p}_{xy2} - 2\mathbf{V}_{txy}\tau - L\omega\tau\mathbf{r}_{xy}'\right) \cdot \left(\boldsymbol{\rho}_{xyn}' - \boldsymbol{\rho}_{xym}'\right)\right] \tag{31}$$

where $\mathbf{r}_{xy}' = (-r_y, r_x)$.

Back to Equation (26), two terms caused by turbulence in the equation can be written as Equations (32) and (33), respectively [22].

$$\begin{aligned}H_1 &= \langle T_n\left(\mathbf{p}_1, -\frac{\tau}{2}\right)T_n^*\left(\mathbf{p}_1, -\frac{\tau}{2}\right)T_m\left(\mathbf{p}_2, \frac{\tau}{2}\right)T_m^*\left(\mathbf{p}_2, \frac{\tau}{2}\right)\rangle \\ &= \exp\left[4C_{\chi i}\left(\boldsymbol{\rho}_{xymn}', \tau\right) + 4C_{\chi R}\left(\boldsymbol{\rho}_{xymn}', \mathbf{p}_{xy-}, \tau\right)\right]\end{aligned} \tag{32}$$

$$\begin{aligned}H_2 &= \langle T_n\left(\mathbf{p}_1, -\frac{\tau}{2}\right)T_n^*\left(\mathbf{p}_2, \frac{\tau}{2}\right)T_m\left(\mathbf{p}_2, \frac{\tau}{2}\right)T_m^*\left(\mathbf{p}_1, -\frac{\tau}{2}\right)\rangle \\ &= \exp\left[2C_{\chi i}(0,0,\tau) - 2C_{\chi i}(0,0,0) + C_{\chi i}\left(\boldsymbol{\rho}_{xymn}', 0, \tau\right) + 2C_{\chi i}\left(\boldsymbol{\rho}_{xymn}', 0, 0\right) + C_{\chi i}\left(\boldsymbol{\rho}_{xymn}', 0, -\tau\right)\right] \\ &\times \exp\left[2C_{\chi R}(0, \mathbf{p}_{xy-}, \tau) - 2C_{\chi R}(0,0,0) + C_{\chi R}\left(\boldsymbol{\rho}_{xymn}', \mathbf{p}_{xy-}, \tau\right) + 2C_{\chi R}\left(\boldsymbol{\rho}_{xymn}', 0, 0\right) + C_{\chi R}\left(\boldsymbol{\rho}_{xymn}', 0, -\tau\right)\right] \\ &\times \exp\left\{-\frac{1}{2}\left[D_i\left(\boldsymbol{\rho}_{xymn}', 0, \tau\right) + D_i\left(\boldsymbol{\rho}_{xymn}', 0, -\tau\right) - 2D_i(0,0,\tau) - 2D_i\left(\boldsymbol{\rho}_{xymn}', 0, 0\right) + D_R\left(\boldsymbol{\rho}_{xymn}', \mathbf{p}_{xy-}, \tau\right)\right]\right\} \\ &\times \exp\left\{-\frac{1}{2}\left[D_R\left(\boldsymbol{\rho}_{xymn}', -\mathbf{p}_{xy-}, -\tau\right) - 2D_R(0, \mathbf{p}_{xy-}, \tau) - 2D_R\left(\boldsymbol{\rho}_{xymn}', 0, 0\right)\right]\right\}\end{aligned} \tag{33}$$

where $\boldsymbol{\rho}_{xymn}' = \boldsymbol{\rho}_{xyn}' - \boldsymbol{\rho}_{xym}'$, $\mathbf{p}_{xy-} = \mathbf{p}_{xy1} - \mathbf{p}_{xy2}$. $D_i(\boldsymbol{\rho}, \mathbf{p}, \tau)$ and $D_R(\boldsymbol{\rho}, \mathbf{p}, \tau)$ are the wave structure functions of the two spherical waves propagating along the forward and backward path respectively, which have the same form shown in Equation (34) because of the principle of reciprocity

$$D_i(\boldsymbol{\rho}, \mathbf{p}, \tau) = D_R(\boldsymbol{\rho}, \mathbf{p}, \tau) = 2.91Lk^2\int_0^1 C_n^2(\xi H)\rho_\xi^{5/3}d\xi \tag{34}$$

$C_{\chi i}(\boldsymbol{\rho}, \mathbf{p}, \tau)$ and $C_{\chi R}(\boldsymbol{\rho}, \mathbf{p}, \tau)$ are the log amplitude covariance functions on the forward and backward path respectively, which have the same form shown in Equation 35

$$\begin{aligned}&C_{\chi i}(\boldsymbol{\rho}, \mathbf{p}, \tau) = C_{\chi R}(\boldsymbol{\rho}, \mathbf{p}, \tau) = 4.3374k^2L \\ &\times \mathrm{Re}\left(\int_0^1 d\xi C_n^2(\xi H)\left\{0.5i^{5/6}(L/k)^{5/6}[\xi(1-\xi)]^{5/6}{}_1F_1\left[-5/6; 1; ik\rho_\xi{}^2/(4L\xi(1-\xi))\right] - 0.1674\rho_\xi{}^{5/3}\right\}\right.\end{aligned} \tag{35}$$

where $\rho_\xi = \left|(\mathbf{p} + \mathbf{v}_w\tau)\xi + (\boldsymbol{\rho} + \mathbf{V}_{xy}\tau)(1-\xi)\right|$, $\mathbf{v}_w$ is the wind speed near the ground. $C_n^2(\xi H)$ is the strength of the atmospheric turbulence as a function of the height above the ground. The model proposed by ITU-R in 2001 is adopted for $C_n^2(\xi H)$ [15].

3. Numerical calculation and analysis

3.1. A fast algorithm for the correlation function of speckle intensity

By substituting Equations (31)–(31)–(33) into Equation (26), the correlation function of speckle intensity becomes Equation 36

$$B_I(\mathbf{p}_1,\mathbf{p}_2,\tau)=\sum_{n=1}^{N}\sum_{m=1}^{N}I_nI_mH_1\left(\boldsymbol{\rho}'_{xyn}-\boldsymbol{\rho}'_{xym}\ ,\ \mathbf{p}_{xy1}-\mathbf{p}_{xy2}\ ,\ \tau\right)$$
$$+\sum_{n=1}^{N}\sum_{m\neq n}^{N}I_nI_m\exp\left[-\frac{ik}{L}\left(\mathbf{p}_{xy1}-\mathbf{p}_{xy2}-2\mathbf{V}_{txy}\tau-L\omega\tau\mathbf{r}'_{xy}\right)\cdot\left(\boldsymbol{\rho}'_{xyn}-\boldsymbol{\rho}'_{xym}\right)\right]H_2\left(\boldsymbol{\rho}'_{xyn}-\boldsymbol{\rho}'_{xym}\ ,\ \mathbf{p}_{xy1}-\mathbf{p}_{xy2}\ ,\ \tau\right) \tag{36}$$

When the number of facets is large, it costs too much time to calculate Equation (36) even using computer programs. For example, when the target is divided into facets, it takes about several hours to tens of hours to solve Equation (36) with a personal computer. In order to speed up the calculation, a fast algorithm is developed to solve Equation (36).

Firstly, the equation is transformed into Equation 37

$$B_I(\mathbf{p}_1,\mathbf{p}_2,\tau)=\sum_{n=1}^{N}I\left(\boldsymbol{\rho}'_{xyn}\right)\sum_{m=1}^{N}I\left(\boldsymbol{\rho}'_{xym}\right)K\left(\boldsymbol{\rho}'_{xyn}-\boldsymbol{\rho}'_{xym}\right)-\sum_{n=1}^{N}I_n^2H_2\left(0\ ,\ \mathbf{p}_{xy1}-\mathbf{p}_{xy2}\ ,\ \tau\right) \tag{37}$$

Where $I(\boldsymbol{\rho}'_{xyn})$ is another form of I_n, and $K(\boldsymbol{\rho}'_{xyn}-\boldsymbol{\rho}'_{xym})$ can be written as Equation 38

$$K\left(\boldsymbol{\rho}'_{xyn}-\boldsymbol{\rho}'_{xym}\right)=H_1\left(\boldsymbol{\rho}'_{xyn}-\boldsymbol{\rho}'_{xym}\ ,\ \mathbf{p}_{xy1}-\mathbf{p}_{xy2}\ ,\ \tau\right)$$
$$+\exp\left[-\frac{ik}{L}\left(\mathbf{p}_{xy1}-\mathbf{p}_{xy2}-2\mathbf{V}_{txy}\tau-L\omega\tau\mathbf{r}'_{xy}\right)\cdot\left(\boldsymbol{\rho}'_{xyn}-\boldsymbol{\rho}'_{xym}\right)\right]H_2\left(\boldsymbol{\rho}'_{xyn}-\boldsymbol{\rho}'_{xym}\ ,\ \mathbf{p}_{xy1}-\mathbf{p}_{xy2}\ ,\ \tau\right) \tag{38}$$

For a group of fixed parameters $(\mathbf{p}_1,\mathbf{p}_2,\tau)$, the term $G(\boldsymbol{\rho}'_{xyn})=\sum_{m=1}^{N}I(\boldsymbol{\rho}'_{xym})K(\boldsymbol{\rho}'_{xyn}-\boldsymbol{\rho}'_{xym})$ in Equation (37) is a typical convolution process, which can be solved by using FFT algorithm. After obtaining the values of $G(\boldsymbol{\rho}'_{xyn})$ for all the facets, the left calculation is a process with the complexity $O(N)$, which can be calculate directly.

3.2. Transient characteristics of the speckle intensity

For speckle field in turbulent environment, the physical quantity that people are more interested in is usually the normalized covariance function defined by Equation 39

$$c(\mathbf{p}_1,\mathbf{p}_2,\tau)=\frac{B_I(\mathbf{p}_1,\mathbf{p}_2,\tau)}{\langle I(\mathbf{p}_1)\rangle\langle I(\mathbf{p}_2)\rangle}-1 \tag{39}$$

where $\langle I(\mathbf{p})\rangle$ is the mean intensity expressed by Equation 40

$$\langle I(\mathbf{p}_1)\rangle=\langle I(\mathbf{p}_2)\rangle=\sum_{n=1}^{N}I_n \tag{40}$$

It can be known from the expression of the correlation function of the speckle intensity that the normalized covariance is a function of $\mathbf{p}_-$ and τ. Here in the paper, the effects of the space and time are discussed separately. First is the variety of the normalized covariance with $\mathbf{p}_-$.

For the simplicity of calculation, we take the cylindrical target with Lambertian surface as the example to calculate the normalized covariance.in the default situation, the wavelength of the laser beam is $\lambda = 1.06\mu$m, the target is just above the laser emitter with the distance between them being $L = 100$km and the axis of the cylinder being along the x axis. the height of the target is $h = 0.6$m, the bottom radius is $r = 0.2$m. The brdf of the Lambertian surface can be written as Equation 41

$$\mathrm{brdf}(\theta_i,0;\theta_i\ ,\quad\pi)=\frac{K}{2\pi} \tag{41}$$

where K is the albedo of the surface.

Then, Equation (39) is calculated by using the fast algorithm while the time parameter is set $\tau = 0$ s.

The distribution of the normalized covariance on the space is shown in Fig. 3. The curves vary with turbulence conditions, target types and the direction of $\mathbf{p}_-$ while all curves decline to certain constants as $|\mathbf{p}_-|$ grows. The larger the size of the target is, the more rapidly the normalized covariance fall along this direction. The effect of turbulence includes three points: (1) when $\mathbf{p}_- \to 0$, the normalized covariance function degenerates to the normalized variance of the speckle intensity $\sigma_I^2 = c(0)$, which reflects the contrast of speckle field. In the presence of turbulence, σ_I^2 is larger than 1, which indicates that the speckle field in turbulence deviates from the complex Gaussian distribution and distributes more dispersedly. (2) When $\mathbf{p}_- \to \infty$, $c(\mathbf{p}_-)$ tends to a value larger than zero and independent to the direction of $\mathbf{p}_-$. The value is called Residual Scintillation Index which indicate the intensity fluctuation of the scattering light as a whole [19]. (3) According to the falling speed of the curves in the presence of turbulence, the speckle field fluctuates at two space scales. One scale is caused by turbulence, which is not related to the strength of turbulence and the size of the target. This scale is about the correlation length of the reflected field by a point target, which is about $l_a = 1.8$ cm under the given conditions [14]. The other scale is the correlation length of the speckle field from the target in vacuum, which is basically independent to turbulence, but it is affected by the size and shape of the target. The second scale can be written as $l_s \approx \lambda L/D$ [21].

Another important phenomenon that can be found in Fig. 3 is that Residual Scintillation Index of a point target is much higher than that of a cylinder. In fact, further calculations show that the larger the target is, the smaller the normalized intensity variance and residual scintillation index are. This phenomenon is called the averaging effect of the target aperture and it is a form of expression of anisoplanatism. A large target can be divided into several parts, the light on and off different parts of the target propagates through unrelated turbulence and fluctuates independently. Light along unrelated paths adds on the receiving plane incoherently, the fluctuation of the intensity on each path are averaged. A larger target contains more independent parts and cause a greater averaging effect. The target aperture averaging factor is defined to measure the effect by

$$A(r,h) = \left(\sigma_I^2 - 1\right) / \left(\sigma_{IMax}^2 - 1\right) \tag{42}$$

where σ_{IMax}^2 is the normalized variance of the speckle intensity from a rough tiny target, for example a 1 mm square plane, under the same condition.

σ_I^2 and σ_{IMax}^2 can be obtained by solving Equation (39), $A(r,h)$ can be evaluated by substitute σ_I^2 and σ_{IMax}^2 into Equation (42) in the cases of targets with different sizes. Fig. 4 shows the curves of equi averaging factor on the $r-h$ plane. In general, the averaging factor decreases with the increase of each dimension while the factor declines a little slower along dimension of the diameter. It can be deduced reasonably that the averaging factor tends to zero when any dimension of the target is large enough.

3.3. Dynamic characteristics of the speckle intensity

Calculating Equation (39) in the case of $\mathbf{p}_- = 0$ m, the temporal distribution of normalized covariance function of the speckle intensity at a single point are obtained. Fig. 5(a) and (b) shows the curves of the temporal covariance function of translating targets and rotating target, respectively. It is found that $c(\tau)$ is a long tail function, which means the curves can also be divided into two parts: the fast falling head and the slow falling tail. That is, the temporal fluctuation of the speckle intensity is also at two scales. The fluctuation on the first time scale is caused by target scattering, which is about the correlation time of the dynamic speckle in vacuum. The second time scale is caused by the relative motion of turbulence across the light path, which is basically not affected by turbulence strength and the rotating motion of the target, but by size and translation velocity of the target as well as speed and direction of the atmospheric wind. When translating motion exists, there is a significant impact of the wind direction on the curve, in which case the second time scale of the speckle field from an extended target is larger than the correlation time of the speckle field from a point target under the same condition (about 0.35 ms). When the direction of the wind is consistent with that of the target motion, the tail of the curve is still longer.

In order to describe the influence of turbulent atmosphere on the normalized covariance more clearly, the second time scale τ_c of the speckle field is defined by Equation 43

$$c(\tau_c) = 0.1\left(\sigma_I^2 - 1\right) \tag{43}$$

that is the time when the covariance caused by turbulence declines to 10 percent of its peak value.

If the target is too small (about H < 0.2 m under the given condition), the first time scale approaches or exceeds the second scale, Equation (43) is invalid; Or if the target is too large (H > 1.2 m), the aperture averaging effect of the target is so strong that the intensity fluctuation caused by turbulence is smoothed out. So, it is necessary to investigate τ_c only for a medium size target. Fig. 6(a) shows how τ_c changes with the size of target in the range of 0.2 m < H < 1.2 m. It can be found that τ_c increases linearly with the growing of the target size when the direction of wind speed is the consistent with the translating direction of the target, and τ_c decreases linearly with the growing target size when the two directions are orthogonal to each other.

The rotating motion of the target basically has no effect on the curves of τ_c in the linear range, however, the rotating motion does reduce the first time scale, which expands the limitation of the linear range to where the target is smaller. Comparing the curves in the

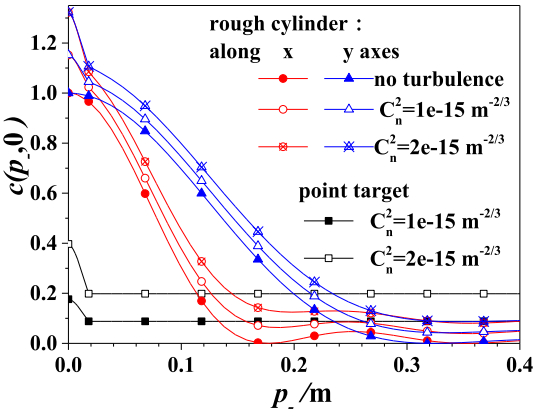

Fig. 3. Normalized covariance of the speckle field from the rough cylinder with space separation.

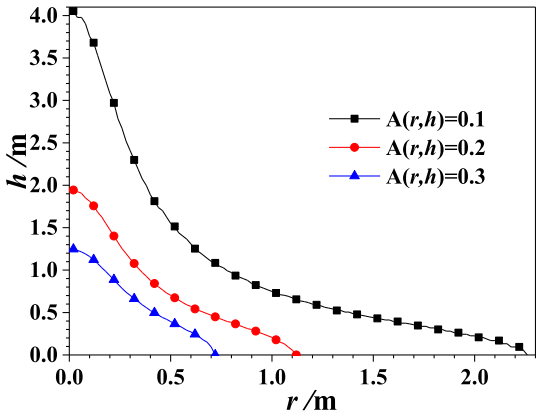

Fig. 4. Equi averaging factor with the variation of the radius and height.

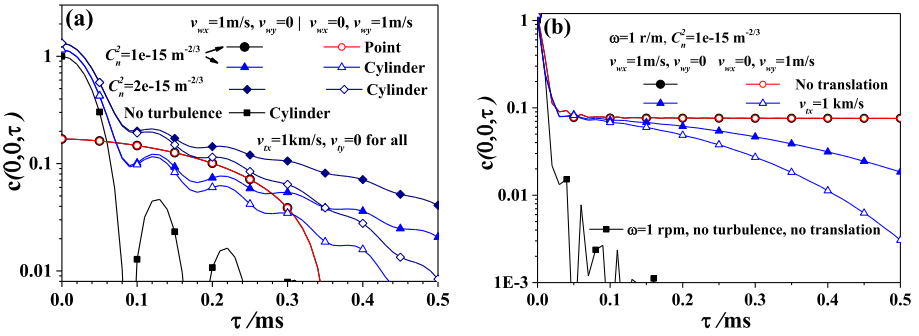

Fig. 5. Normalized covariance of the speckle field from the rough cylinder with time separation, where the label "Point" indicates the target is a point scatter, "Cylinder" indicates the cylindrical target. (a) translating target, (b) rotating target.

cases of different translating speed, it is found that the second time scale is inversely proportional to the translating speed. As the first time scale has the same relation with the translating speed when no rotation exits, it can be deduced that the main shape of the normalized covariance function does not change with the moving speed of the target.

Fig. 6 (b) shows the influence of wind speed and direction (expressed by θ, the angle between wind direction and target translational direction) on τ_c. When the wind speed is above a minimum (about 0.05 m/s), τ_c decreases slowly and linearly with the increase of wind speed. The influence of wind direction on τ_c is more significant than its speed, the closer is θ to 90° (the case that the wind direction is orthogonal to the translating direction of the target), the smaller τ_c is. For the winds from two opposite directions, τ_c is smaller when moving downwind, however, the differences of τ_c respectively under the downwind and upwind conditions are quite small.

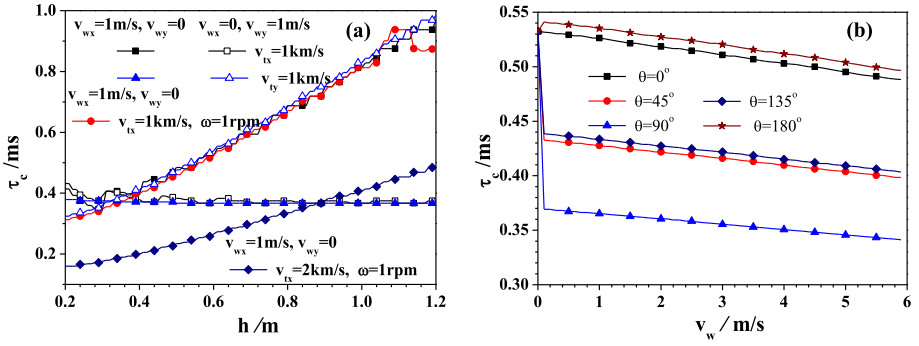

Fig. 6. The second time scale of the normalized covariance function. (a)with the height of the cylinder; (b)with the wind speed.

4. Conclusion

The core of the results in the paper is obtaining the formula of the spatiotemporal correlation function of laser speckle intensity from a 3D target, which can be used to study the spatial and temporal characteristics of intensity fluctuation of the speckle field in vacuum or turbulent environment. Considering that the spatiotemporal characteristics of speckle field in vacuum have been analyzed and summarized in existing literatures, this paper focuses on the particularity of the temporal and spatial fluctuation of speckle field in atmospheric turbulence. Numerical results are obtained by taking cylindrical targets as examples, but the conclusions are applicable to most 3D targets.

The particularity of speckle field from a 3D target in turbulent atmospheric environment is reflected in the following points:

(1) The speckle field deviates from the Gaussian distribution, which is reflected in the normalized intensity variance that is greater than 1.
(2) There is residual scintillation in the speckle field, which is reflected in the phenomenon that the normalized intensity covariance does not tend to zero when the spacing of the two points increases.
(3) Aperture averaging effect of the target exits, that is, the larger the target size, the closer the normalized intensity variance is to 1 and the weaker the residual scintillation phenomenon. The above points are consistent with the results in literatures, which are extended to general types of targets in this paper.
(4) Temporal fluctuation of the speckle intensity also shows two scales. One time scale is about equal to the correlation time of vacuum speckle intensity fluctuation, and the second time scale is about the correlation time of intensity fluctuation caused by turbulence. The second time scale is greatly affected by translating velocity of the target and direction of the wind, and slightly influenced by the target size and wind speed.

Traditional research on the scattered light by targets in turbulent atmosphere usually uses the separation the spatial and temporal scales caused by different factors, so as to realize the respective researches on the effects of turbulence and targets. However, the results of this paper show that the scales of the speckle fluctuation do not necessarily differ greatly in space and time, in which case, the speckle fluctuation caused by the factors must be studied as a whole. The greatest significance of this paper is to provide a feasible tool for research of this kind.

Author contribution statement

Wang Liguo: Conceived and designed the experiments; Wrote the paper.
Gong Lei & Yang Lihong: Performed the experiments.
Li Yaqing & Li Yao: Analyzed and interpreted the data.
Yang Zhiqiang: Contributed reagents, materials, analysis tools or data.

Funding statement

Yaqing Li and Yao Li were supported by National Natural Science Foundation of China [61805190 & 62001364].
Lei Gong was supported by Scientific Research Plan Projects of Shaanxi Education Department [20JS059], Xi'an Technological University principal foundation key projects [XPY200206].

Data availability statement

Data included in article/supp. material/referenced in article.

Declaration of interest's statement

The authors declare no competing interests.

References

[1] J. Bertolotti, E.V. Putten, C. Blum, A. Lagendijk, W.L. Vos, A.L. Mosk, Non-invasive imaging through opaque scattering layers, Nature 491 (2015) 232, https://doi.org/10.1038/nature11578.
[2] N. Takai, T. Iwai, Real-time velocity measurement for a diffuse object using zero-crossings of laser speckle, J. Opt. Soc. Am. 70 (1980) 450–455, https://doi.org/10.1364/JOSA.70.000450.
[3] J. Zhang, J.X. Zhang, X.D. Ma, Deformation measurement technology of large airfoil based on digital speckle, China Measure. Test 47 (2021) 149–155, in Chinese, https://kns.cnki.net/kcms/detail/detail.aspx?FileName=SYCS202102023&DbName=CJFQ2021.
[4] J.W. Goodman, Speckle Phenomena in Optics: Theory and Applications, Greenwood Village: Roberts and Company, 2007, https://doi.org/10.1117/3.2548484.
[5] H.J. Rabal, R.A. Braga, Dynamic Laser Speckle and Applications, CRC Press, Boca Raton, 2010, https://doi.org/10.1201/9781315219080.
[6] W.K. Gao, X.P. Du, Y. Wang, B.Y. Yang, Review of laser speckle target detection technology, Chin. Opt. 13 (2020) 1182–1193, in Chinese, http://chineseoptics.net.cn/cn/article/doi/10.37188/CO.2020-0049.
[7] H.T. Yura, S.G. Hanson, M.J. Jakobsen, Speckle dynamics resulting from multiple interfering beams, JOSA 25 (2008) 318–326, https://doi.org/10.1364/JOSAA.25.000318.

[8] G. Zhang, Statistical Properties of Laser Speckle from Rough Objects and Analysis on Micro-motion Characteristic. Ph.D. Dissertation, Xidian University, Xi'an, 2013 in Chinese, https://kns.cnki.net/KCMS/detail/detail.aspx?dbname=CDFD1214&filename=1013297798.nh.
[9] T.J. Sun, C.F. Cheng, Temporal and spatial coherence properties of ultrafast laser speckle fields, J. Shanxi Normal Univ. 32 (2017) 52–55, in Chinese, https://www.nstl.gov.cn/paper_detail.html?id=68719da31cb640d7dc8280bbb59a2927.
[10] J.C. Dainty, J.W. Goodman, et al., Laser Speckle and Related Phenomena, Springer Berlin Heidelberg, 1975. https://link.springer.com/book/10.1007/978-3-662-43205-1.
[11] J.F. Holmes, M.H. Lee, J.R. Kerr, Effect of the log-amplitude covariance function on the statistics of speckle propagation through the turbulent atmosphere, JOSA 70 (1980) 355–360, https://doi.org/10.1364/JOSA.70.000355.
[12] V.S.R. Gudimetla, J.F. Holmes, Probability density function of the intensity for a laser-generated speckle field after propagation through the turbulent atmosphere, JOSA 72 (1982) 1213–1218, https://doi.org/10.1364/JOSA.72.001213.
[13] V.P. Aksenov, V.A. Banakh, V.L. Mironov, Fluctuations of retroreflected laser radiation in a turbulent atmosphere, JOSA.A 1 (1984) 263–274, https://doi.org/10.1364/JOSAA.1.000263.
[14] L.C. Andrews, R.L. Phillips, Laser Beam Propagation through Random Media, second ed., SPIE Press, Bellingham, 2005 https://doi.org/10.1117/3.626196.
[15] H.Y. Wei, Z.S. Wu, H. Peng, Scattering from a diffuse target in the slant atmospheric turbulence, Acta Phys. Sin. 57 (2008) 6666–6672, https://doi.org/10.7498/aps.57.6666, in Chinese.
[16] J. Li, M.P. Gordon, O. Korotkova, Enhanced Back-Scatter in double-pass optical links with non-classic turbulence, Opt Express 26 (2018) 10128–10139, https://doi.org/10.1364/OE.26.010128.
[17] O. Korotkova, Enhanced backscatter in LIDAR systems with retro-reflectors operating through a turbulent ocean, JOSA.A 35 (2018) 1797–1804, https://doi.org/10.1364/JOSAA.35.001797.
[18] L.G. Wang, Y.Q. Li, M. Gao, L. Gong, Fluctuations of light intensity scattered from multiple glints in atmospheric turbulence, Proc. SPIE 9796 (2016) 97960E, https://doi.org/10.1117/12.2229815.
[19] L.G. Wang, M. Gao, Y.Q. Li, L. Gong, Intensity fluctuations of reflected wave from a diffuse target with a hard edge in atmospheric turbulence, J. Quant. Spectrosc. Radiat. Transfer 195 (2017) 141–146, https://doi.org/10.1016/j.jqsrt.2016.12.027.
[20] L.G. Wang, Y.Q. Li, L. Gong, Q. Wang, Intensity fluctuations of reflected wave from distributed particles illuminated by a laser beam in atmospheric turbulence, J. Quant. Spectrosc. Radiat. Transfer 224 (2019) 355–360, https://doi.org/10.1016/j.jqsrt.2018.11.036.
[21] G. Zhang, Z.S. Wu, Fluctuation correlation of the scattered intensity from two-dimensional rough surfaces, Opt Express 20 (2012) 1491, https://doi.org/10.1364/OE.20.001491.
[22] L.G. Wang, Characteristics of Reflected Wave from Targets Illuminated by Laser Beams in Turbulent Atmosphere. Ph.D. Dissertation, Xidian University, Xi'an, 2014 in Chinese, https://kns.cnki.net/KCMS/detail/detail.aspx?dbname=CDFDLAST2015&filename=1014324956.nh.